Applied Physics Letters

A 30-nm thick integrated hafnium zirconium oxide nano-electro-mechanical membrane resonator

Cite as: Appl. Phys. Lett. **116**, 043501 (2020); https://doi.org/10.1063/1.5134856
Submitted: 09 November 2019 . Accepted: 17 January 2020 . Published Online: 27 January 2020

M. Ghatge, G. Walters, T. Nishida, and R. Tabrizian

Applied Physics Letters ARTICLE scitation.org/journal/apl

A 30-nm thick integrated hafnium zirconium oxide nano-electro-mechanical membrane resonator

Cite as: Appl. Phys. Lett. **116**, 043501 (2020); doi: 10.1063/1.5134856
Submitted: 9 November 2019 · Accepted: 17 January 2020 ·
Published Online: 27 January 2020

M. Ghatge,[a] G. Walters, T. Nishida, and R. Tabrizian

AFFILIATIONS

Electrical and Computer Engineering Department, University of Florida, Gainesville, Florida 32611, USA

[a]Electronic mail: ruyam@ufl.edu

ABSTRACT

This paper reports a 30 nm-thick integrated nano-electro-mechanical resonator based on atomically engineered ferroelectric hafnium zirconium oxide ($Hf_{0.5}Zr_{0.5}O_2$) film. A 10 nm-thick $Hf_{0.5}Zr_{0.5}O_2$ layer is atomically engineered through capping with 10 nm-thick titanium nitride (TiN) layer and rapid thermal annealing to promote the orthorhombic crystal phase with strong ferroelectric properties. The resulting metal-ferroelectric-metal (MFM) membrane is then patterned to create an integrated nano-electro-mechanical resonator with an overall thickness of 30 nm and a planar-to-vertical aspect ratio exceeding 10^4:1. Benefiting from large electrostrictive effects in ferroelectric $Hf_{0.5}Zr_{0.5}O_2$, the 30 nm-thick nanomechanical resonator is excited into flexural resonance at 195 kHz with a very large vibration amplitude of ~100 nm. The transmission response of the nano-electro-mechanical resonator is extracted, using a two-port apodization of the TiN electrodes, showing quality factors (Q) of 15 and 3300 at atmospheric and 10^{-7} Torr ambient pressures, respectively. Finally, the structural robustness of the MFM nano-membrane is explored through the application of a ~24 μm deflection, using a point-force by a micro-probe, highlighting the extended elasticity despite the small thickness and ultra-high aspect ratio. The atomic-level thickness, fully integrated operation, high Q, and structural robustness of the $Hf_{0.5}Zr_{0.5}O_2$-based nano-membrane resonator promise its potential for the realization of highly integrated transducers for chip-scale classical and quantum information processing and sensing applications.

Harnessing high quality-factor (Q) mechanical resonance at the nanoscale enables the realization of ultra-high-resolution sensors and actuators and extreme frequency scaling of radio frequency oscillators and spectral processors. Offering Qs that are several orders of magnitude higher than its electrical counterparts and frequencies that only increase with their physical miniaturization, nanomechanical resonators offer a transforming solution to the emerging need for cm- and mm-wave spectral processing in wireless systems.[1–3] Furthermore, the vanishingly small dimensions of the nanomechanical resonator enable a physical interaction with the external world at the atomic level.[4] This, besides the high-Q frequency selection that enables inherent cooling of the background noise, places nanomechanical resonators in a prominent position for the realization of ultra-high-resolution transducers for classical and quantum sensing applications.[5,6]

Over the past decade, the creation of resonant nanomechanical devices has been followed through the use of various nano-structures including silicon cantilever nano-beams, atomically thin two-dimensional crystals, and carbon nanotubes.[7–9] These approaches have exploited geometrical and material engineering of the nano-structure to ensure the existence of a high-Q natural mechanical resonance at a desirable frequency. The resulting high-Q mechanical resonance has been measured using a variety of approaches such as thermal excitation, optical interrogation, and magnetic/hall-effect transduction.[9–11] While successful in harnessing the dynamics of high-frequency and high-Q mechanical resonance, these transduction approaches commonly suffered from the incompatibility for chip-scale/monolithic integration necessary for practical applications.

Atomic-layered hafnia-based films have recently emerged as potential candidates for the realization of integrated electromechanical transduction at the nanoscale.[12] Since the discovery of ferroelectric properties in atomically engineered hafnia in 2011, a wide spectrum of research and development efforts have been focused on exploiting hafnia-based films for the realization of ultra-low-power non-volatile memories and field-effect transistors.[13,14]

Recently, electrostrictive electromechanical transduction has been demonstrated in atomic-layered ferroelectric hafnium zirconium oxide ($Hf_{0.5}Zr_{0.5}O_2$) films and used for the integrated excitation of mechanical resonance in silicon (Si) and aluminum nitride (AlN) membranes.[12,15] In these works, thick Si and AlN layers are used to enhance the structural robustness of the device and alleviate the challenges with nanomechanical resonator fabrication. However, the addition of thick Si/AlN layers substantially reduces the inherent figures of

merits of the atomically thin $Hf_{0.5}Zr_{0.5}O_2$ transducers by loading the electromechanical coupling efficiency of the transduction and preventing the extreme frequency scaling of the resonator due to the inverse proportionality of the resonance frequency of the bulk acoustic mode with the overall resonator thickness.

This Letter demonstrates an atomically thin nanomechanical resonator that is realized entirely from the $Hf_{0.5}Zr_{0.5}O_2$ transducer and without the use of any thick structural layer. Such an architecture substantially enhances the electromechanical coupling of the resonator and enables fully integrated electrical excitation and readout of the mechanical resonance dynamics, without the need for optical interrogation. Furthermore, the resonators presented in this work enable the evaluation of electromechanical dissipation mechanisms in $Hf_{0.5}Zr_{0.5}O_2$ transducers through the exploration of the nanomechanical resonator Q. This study will serve toward the identification of the fundamental limitations in adoption of $Hf_{0.5}Zr_{0.5}O_2$-based nanomechanical resonators in integrated oscillators, filters, and resonant sensors.

The $Hf_{0.5}Zr_{0.5}O_2$-based metal-ferroelectric-metal (MFM) membrane resonators are created by sandwiching a 10 nm-thick $Hf_{0.5}Zr_{0.5}O_2$ transducer film between two 10 nm-thick titanium nitride (TiN) electrodes. A two-port doubly clamped 195 kHz resonator with a planar-to-vertical aspect ratio exceeding 10^4:1 and a vibration amplitude of ~100 nm is demonstrated with a large Q of 3300, when measured at 10^{-7} Torr ambient pressure. Electrical and optical characterization techniques are used to demonstrate the frequency response, vibrational mode of operation, and ferroelectric behavior of the device.

Ultrathin $Hf_{0.5}Zr_{0.5}O_2$ films grown by atomic layer deposition (ALD) are amorphous in nature due to the low thermal budget of the growth process. However, the film is deliberately driven into crystallinity with TiN capping electrodes and rapid thermal annealing (RTA) to achieve a predominant non-centrosymmetric orthorhombic phase that exhibits a strong ferroelectricity.[15] Figure 1 shows the cross-sectional transmission electron microscopy (XTEM) image of the MFM stack and the ferroelectric response of the transducer. Figure 1(b) highlights the predominant orthorhombic crystal phase in a polycrystalline $Hf_{0.5}Zr_{0.5}O_2$ film through fast Fourier transform (FFT). Figure 1(c) confirms the ferroelectric nature of the film through the polarization-electric field (P-E) hysteresis curve. A remnant polarization (P_r) of ~15 $\mu C/cm^2$ is observed for the 10 nm $Hf_{0.5}Zr_{0.5}O_2$ film. The fabrication process for the realization of the 30 nm-thick membrane resonator is summarized in the supplementary material.

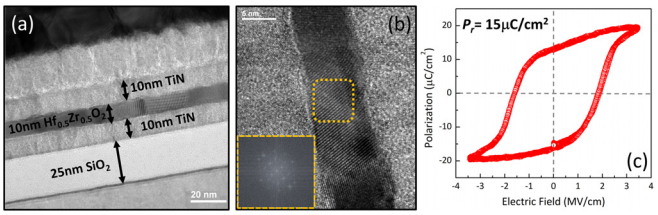

FIG. 1. (a) XTEM image of the resonator stack-TiN/$Hf_{0.5}Zr_{0.5}O_2$/TiN on top of SiO_2. (b) Zoomed-in view of the ferroelectric $Hf_{0.5}Zr_{0.5}O_2$ film showing the atomic diffraction patterns of the polycrystalline film. The inset shows the FFT of the region highlighted, demonstrating a predominant orthorhombic crystal phase. (c) Measured polarization-electric field hysteresis response of the $Hf_{0.5}Zr_{0.5}O_2$ film acting as a transducer for the resonator shows a remnant polarization of ~15 $\mu C/cm^2$.

Surface losses are a major source of energy dissipation in nano-electro-mechanical resonators, and thus, imperfect thin films with surface defects play a major role in degrading the resonator performance.[16] Thus, all films are grown via ALD to achieve good uniformity, minimal surface roughness and defects, and thickness-precision required for the resonator design. Figure 2 shows the scanning electron microscopy (SEM) image of the doubly clamped nano-electro-mechanical resonator. With a length of ~500 μm and a thickness ~30 nm, the robust mechanical properties of the MFM membrane are evident as the planar-to-vertical aspect ratio exceeds over 10^4:1. Patterning the top and bottom TiN layers causes the device to warp down at the edges due to the unsymmetrical stack at the top and bottom surfaces, as shown in Fig. 2(a). A bending test performed by applying a point force using a micro-probe in the center of the device is demonstrated in the ion-beam image shown in Fig. 2(b) (Multimedia view). An out-of-plane vertical deflection of ~24 μm is sustained by the device without altering the device performance, indicating the structural robustness of the $Hf_{0.5}Zr_{0.5}O_2$ based MFM nano-electro-mechanical resonator. As the micro-probe continues to deflect the resonator in the out-of-plane direction, the device bends in the opposite direction compared to the equilibrium state shown in Fig. 2(a) before it ruptures as the deflection goes beyond ~26 μm. This huge deflection highlights the extended elasticity of the MFM stack despite the nanoscale thickness and ultra-high aspect ratio of the doubly clamped resonator. Figure 3 shows the out-of-plane flexural mode of vibration of the nano-electro-mechanical resonator captured using holographic microscopy and demonstrated using a vibration amplitude contour map [Fig. 3(a)] and a profile plot across the device length [Fig. 3(b)]. The captured mode-shape shows out-of-plane vibration amplitude as high as ~100 nm (10 × the $Hf_{0.5}Zr_{0.5}O_2$ film thickness) while operating in the linear regime verifying the robust elastic performance of the MFM resonator.

Apart from robust structural characteristics, the $Hf_{0.5}Zr_{0.5}O_2$ based MFM resonator shows promising performance metrics such as high-Q and fully integrated electromechanical excitation and readout. The MFM resonator is characterized, using optical and electrical RF characterization setups, to identify the vibration dynamics in time and

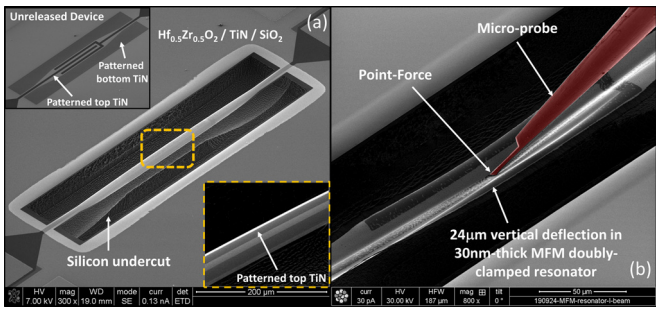

FIG. 2. (a) SEM image of the doubly clamped resonator based on TiN/$Hf_{0.5}Zr_{0.5}O_2$/TiN with an aspect ratio exceeding 10^4:1. The device with such a high aspect ratio warps due to the unsymmetrical nature of the stack. The inset (top left) shows the unreleased device. Bottom TiN is patterned to avoid TiN undercut during the release as discussed in the supplementary material. The inset (bottom right) shows the zoomed-in view of the central electrode region with patterned top TiN. (b) Ion-beam image of the device bent by ~24 μm via applying a point-force using a micro-probe signifying the mechanical robustness of the device. Multimedia view: https://doi.org/10.1063/1.5134856.1

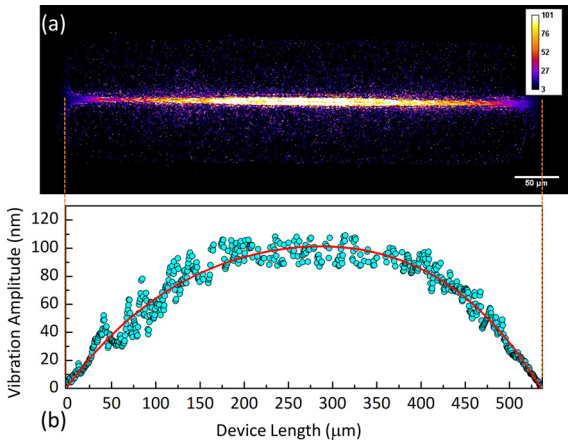

FIG. 3. (a) Contour map of the vibrational amplitude of the entire device captured using holographic microscopy. The device is shown in the central region with the color gradients demonstrating vibration amplitude across the device. Regions with no vibrational response are resolved in darker shades in the contour map. (b) The profile plot of the vibrating device shown underneath the contour map confirms the out-of-plane flexural mode of vibration. The red curve shows the fitted mode-shape profile of the device.

frequency domains over a wide range of ambient pressures. Figure 4 summarizes the characterization results. Figs. 4(a) and 4(b) show the optically measured vibration amplitude of the device in air and moderate vacuum ($P = 800$ mTorr) conditions, respectively. The device is actuated by the application of a stroboscopic sinusoidal input signal to the top TiN electrode, and the time-domain vibration responses are captured optically using a synchronized holographic microscope [Figs. 4(a) and 4(b)]. For the same stroboscopic time-frequency interrogation setup, the broader vibration amplitude envelope around the resonance frequency and the lower vibration amplitude in air [Fig. 4(a)] compared to the response under moderate vacuum conditions [Fig. 4(b)] exhibit air-damping as the dominant dissipative process in mechanical resonance dynamics. This is also evident in the extracted frequency responses in air and moderate vacuum [Figs. 4(c) and 4(d)], showing over two orders of magnitude increase in Q, from ∼15 (in air) to ∼2330 at 800 mTorr ambient pressures. The pressure dependence of the resonance frequency is also evident with ∼6% upward drift in the resonance frequency from 183 kHz in air to 195 kHz at 800 mTorr pressure. Figure 4(e) shows an all-electrical 2-port transmission response of the device measured using a network analyzer demonstrating a Q of ∼3300 at 10^{-7} Torr pressure. The device performance can be significantly improved by opting for a highly conductive electrode material, improving electrode and probing configurations to further reduce the resistive load, and enhancing electromechanical transduction efficiency.

Finally, Fig. 4(f) summarizes the pressure dependence of the nano-mechanical resonator Q over the pressure range of 10^{-7} Torr to 760 Torr. Air damping is a prominent energy dissipation mechanism observed at such low frequencies of operation.[17,18] With thicknesses on the order of few tens of nanometers, the mean free path of the air molecules is much higher than the device dimensions, and thus, its collision with the vibrating device leads to significant energy dissipation.[19] The resulting air-damping Q is given by[20]

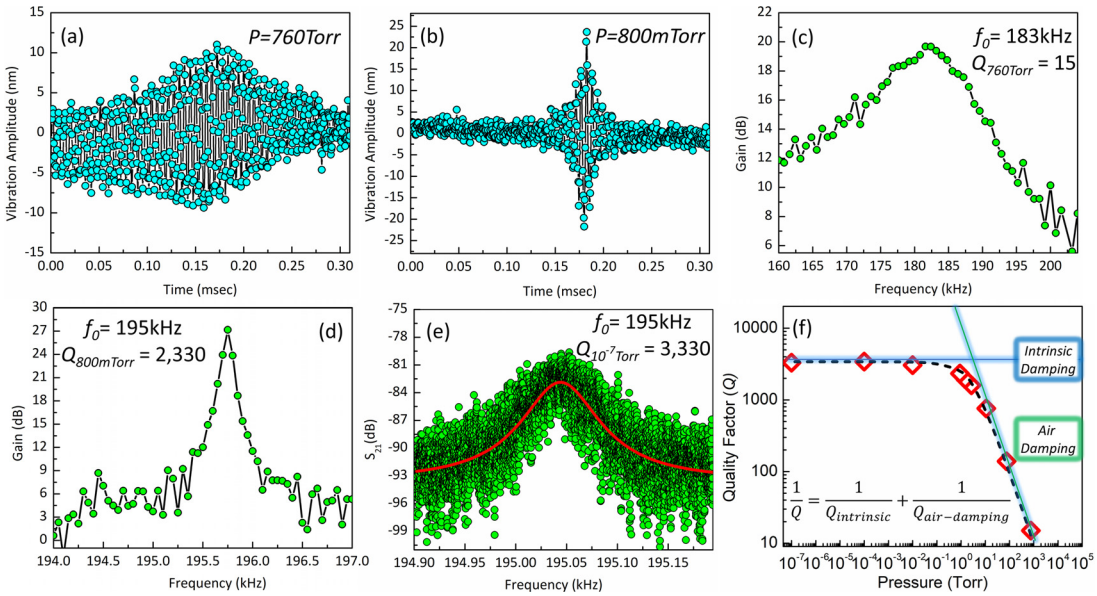

FIG. 4. Captured out-of-plane vibrational amplitude of the device (a) in air and (b) under 800 mTorr ambient pressures. Optically measured frequency response of the device (c) in air showing a $Q_{760\ Torr} \sim 15$ while and (d) under 800 mTorr showing over two-orders of magnitude improvement to ∼2330. (e) 2-port frequency measurement of the device using a network analyzer shows a high-Q of 3300 measured at 10^{-7} Torr resolved using the fitted Lorentzian function (red curve). (f) Quality-factor–pressure relation shows a modified power law relation. The green line shows the $Q_{air\text{-}damping}$, limit while the blue line shows the intrinsic limit of ∼3400 of the presented $Hf_{0.5}Zr_{0.5}O_2$ based MFM nano-electro-mechanical resonator.

$$Q_{air-damping} = \frac{{k_n}^2}{k_m P}\left(\frac{t}{l}\right)^2\left(\frac{\rho E}{12}\right)^{1/2}, \quad (1)$$

where k_n is a constant corresponding to the nth flexural resonance mode,[21] $t, l, \rho, and\ E$ are the thickness, length, density, and elastic modulus of the membrane, respectively, P is the pressure, and k_m is the damping coefficient given by $(32M/9\pi RT)^{1/2}$. Here, M is the mass of the gas molecule, R is the gas constant, and T is the absolute temperature. With out-of-plane flexural mode resonance frequency for a doubly clamped resonator proportional given by $(f_0 \propto (t/l)^2(E/\rho)^{1/2})$,[22] $Q_{air-damping}$ in Eq. (1) is related to the resonance frequency and environmental pressures as

$$Q_{air-damping} \propto \frac{f_0 {k_n}^2 \rho}{k_m P}. \quad (2)$$

Therefore, the overall Q can be formulated as[20]

$$Q = \left(Q_{intrinsic}^{-1} + Q_{air-damping}^{-1}\right)^{-1} = \left(Q_{intrinsic}^{-1} + \alpha_0 P\right)^{-1}, \quad (3)$$

where $Q_{intrinsic}$ reflects the pressure-independent intrinsic dissipation mechanisms and α_0 is a constant related to the resonator physical characteristics and ambient gas properties, according to Eqs. (1) and (2). Equation (3) is used to identify the $Q_{intrinsic}$ of the nanomechanical resonator through curve fitting [Fig. 4(f)]. The analytical curve, according to the Eq. (3) formulation of Q, fits well to the measured data, yielding a $Q_{intrinsic}$ of 3400. Such a large intrinsic Q is significantly higher compared to the 2D-crystal nano-resonators and nano-cantilevers with similar thickness.[19,23–25]

In conclusion, this paper demonstrates the thinnest ever-reported integrated nano-electro-mechanical resonator using a 10 nm-thick ferroelectric $Hf_{0.5}Zr_{0.5}O_2$ film sandwiched between 10 nm-thick top and bottom TiN electrodes. The device operates in the out-of-plane flexural mode of vibration and demonstrates a high-Q of 3300 at 195 kHz, when measured at 10^{-7} Torr pressure. The structural robustness of the 30 nm-thick nano-membrane with an ultra-high planar-to-vertical aspect ratio of 10^4:1 is verified through point-force deflection characterization. The effect of air-damping on Q and resonance frequency is studied across a wide range of pressure values highlighting a modified power-law relationship between Q and pressure. A large intrinsic Q of 3400 is extracted comparing the analytical formulation and measured values. The extreme miniaturization capability to atomic-level thicknesses, fully integrated operation, high-Q, and high mechanical robustness highlights the potential of $Hf_{0.5}Zr_{0.5}O_2$-based nano-electro-mechanical resonators to serve as the integrated transducer for chip-scale classical and quantum information processing and sensing applications.

See the supplementary material for the fabrication process used for the realization of the 30 nm-thick metal-ferroelectric-metal nano-electro-mechanical membrane resonator discussed in this Letter.

The authors would like to thank Nicolas Rudawski for help with TEM and Ion Beam images. The authors would also like to thank the Nanoscale Research Facility for fabrication and characterization facilities. This work was supported in part by NSF Grant Nos. ECCS 1610387 and ECCS 1752206.

REFERENCES

[1]J. Moser, A. Eichler, J. Güttinger, M. I. Dykman, and A. Bachtold, "Nanotube mechanical resonators with quality factors of up to 5 million," Nat. Nanotechnol. **9**(12), 1007 (2014).
[2]S. Kong, S. Zhou, Z. Nie, and K. Wang, "The size-dependent natural frequency of Bernoulli–Euler micro-beams," Int. J. Eng. Sci. **46**(5), 427–437 (2008).
[3]A. Castellanos-Gomez, R. van Leeuwen, M. Buscema, H. S. van der Zant, G. A. Steele, and W. J. Venstra, "Single-layer MoS2 mechanical resonators," Adv. Mater. **25**(46), 6719–6723 (2013).
[4]Y. T. Yang, C. Callegari, X. L. Feng, K. L. Ekinci, and M. L. Roukes, "Zeptogram-scale nanomechanical mass sensing," Nano Lett. **6**(4), 583–586 (2006).
[5]A. Boisen, S. Dohn, S. S. Keller, S. Schmid, and M. Tenje, "Cantilever-like micromechanical sensors," Rep. Prog. Phys. **74**(3), 036101 (2011).
[6]A. Benyamini, A. Hamo, S. V. Kusminskiy, F. von Oppen, and S. Ilani, "Real-space tailoring of the electron–phonon coupling in ultraclean nanotube mechanical resonators," Nat. Phys. **10**(2), 151 (2014).
[7]X. Li, T. Ono, Y. Wang, and M. Esashi, "Ultrathin single-crystalline-silicon cantilever resonators: Fabrication technology and significant specimen size effect on Young's modulus," Appl. Phys. Lett. **83**(15), 3081–3083 (2003).
[8]A. K. Huttel, G. A. Steele, B. Witkamp, M. Poot, L. P. Kouwenhoven, and H. S. van der Zant, "Carbon nanotubes as ultrahigh quality factor mechanical resonators," Nano Lett. **9**(7), 2547–2552 (2009).
[9]J. S. Bunch, A. M. Van Der Zande, S. S. Verbridge, I. W. Frank, D. M. Tanenbaum, J. M. Parpia, and P. L. McEuen, "Electromechanical resonators from graphene sheets," Science **315**(5811), 490–493 (2007).
[10]A. Rahafrooz and S. Pourkamali, "Active self-Q-enhancement in high frequency thermally actuated M/NEMS resonators," in *IEEE 24th International Conference on Micro Electro Mechanical Systems* (IEEE, 2011), pp. 760–763.
[11]D. Paci, F. Pieri, P. Toscano, and A. Nannini, "A CMOS-compatible, magnetically actuated resonator for mass sensing applications," Sens. Actuators, B **129**(1), 10–17 (2008).
[12]M. Ghatge, G. Walters, T. Nishida, and R. Tabrizian, "A nano-mechanical resonator with 10 nm hafnium-zirconium oxide ferroelectric transducer," in *IEEE International Electron Devices Meeting (IEDM)* (IEEE, 2018), pp. 4–6.
[13]T. S. Böscke, J. Müller, D. Bräuhaus, U. Schröder, and U. Böttger, "Ferroelectricity in hafnium oxide thin films," Appl. Phys. Lett. **99**(10), 102903 (2011).
[14]T. Mikolajick, S. Slesazeck, M. H. Park, and U. Schroeder, "Ferroelectric hafnium oxide for ferroelectric random-access memories and ferroelectric field-effect transistors," MRS Bull. **43**(5), 340–346 (2018).
[15]M. Ghatge, G. Walters, T. Nishida, and R. Tabrizian, "An ultrathin integrated nanoelectromechanical transducer based on hafnium zirconium oxide," Nat. Electron. **2**(11), 506–512 (2019).
[16]K. Y. Yasumura, T. D. Stowe, E. M. Chow, T. Pfafman, T. W. Kenny, B. C. Stipe, and D. Rugar, "Quality factors in micron-and submicron-thick cantilevers," J. Microelectromech. Syst. **9**(1), 117–125 (2000).
[17]S. S. Verbridge, R. Ilic, H. G. Craighead, and J. M. Parpia, "Size and frequency dependent gas damping of nanomechanical resonators," Appl. Phys. Lett. **93**(1), 013101 (2008).
[18]O. Svitelskiy, V. Sauer, N. Liu, K. M. Cheng, E. Finley, M. R. Freeman, and W. K. Hiebert, "Pressurized fluid damping of nanoelectromechanical systems," Phys. Rev. Lett. **103**(24), 244501 (2009).
[19]K. L. Ekinci and M. L. Roukes, "Nanoelectromechanical systems," Rev. Sci. Instrum. **76**(6), 061101 (2005).
[20]F. R. Blom, S. Bouwstra, M. Elwenspoek, and J. H. J. Fluitman, "Dependence of the quality factor of micromachined silicon beam resonators on pressure and geometry," J. Vacuum Sci. Technol., B **10**(1), 19–26 (1992).
[21]S. P. Timoshenko, D. H. Young, and W. Weaver, *Vibration Problems in Engineering*, 4th ed. (Wiley, New York, 1974), pp. 415–431.
[22]S. D. Senturia, *Microsystem Design* (Springer Science & Business Media, 2007).
[23]J. Lee, Z. Wang, K. He, J. Shan, and P. X. L. Feng, "Air damping of atomically thin MoS_2 nanomechanical resonators," Appl. Phys. Lett. **105**(2), 023104 (2014).
[24]M. Li, H. X. Tang, and M. L. Roukes, "Ultra-sensitive NEMS-based cantilevers for sensing, scanned probe and very high-frequency applications," Nat. Nanotechnol. **2**(2), 114 (2007).
[25]J. Lee, Z. Wang, K. He, J. Shan, and P. X. L. Feng, "High frequency MoS_2 nanomechanical resonators," ACS Nano **7**(7), 6086–6091 (2013).